

Self-Noise Spectra for 34 Common Electromagnetic Seismometer/Preamplifier Pairs

by Peter W. Rodgers

Abstract Because of a lack of such information, computed self-noise spectra are presented for a total of 34 frequently used electromagnetic-seismometer/preamplifier combinations. For convenience, most of these data are given in three sets of units. Peterson's Low Noise Model is included on each plot for comparison. The self noises of nine frequently employed electromagnetic seismometers properly matched to their operational amplifier (op-amp) preamplifiers are plotted. In terms of amplitude density spectra in $(\text{m}/\text{sec}^2)/\text{Hz}^{0.5}$, the values of the self-noise spectra at resonance range from a low of 3×10^{-10} for the GS-13 to a high of 1.3×10^{-8} for the HS-1. Between these two seismometers, in order of increasing noise at resonance, are the SV-1, SL-210V, S-13, SS-1, L-4C, S-6000CD, and the L-22D.

To show which seismometers exhibit the lowest noise with which operational amplifier preamplifiers, the self noises of the HS-1, L-22D, L-4C, GS-13, SV-1, and SL-210V are plotted each paired with four commonly used op-amps: the LT1028, OP-227, OP-77, and the LT1012. For the GS-13, the LT1012 was the quietest. For the rest, the OP-227 was the best. For a given seismometer, the differences in self noise between op-amps were frequently a factor of 2 or 3, and as large as 10 in one case. The use of these op-amps in the analog front ends of five current digital seismic recorders is discussed.

Introduction

The dynamic range for an electromagnetic (EM) seismometer in combination with its necessary electronic preamplifier is set at the high level by electrical, or sometimes mechanical, saturation (clipping) and at the lowest level by the self noise (or noise floor) of the seismometer/preamplifier combination. To determine the dynamic range, both of these quantities must be known. The upper, electrical saturation level can be obtained from the parameters in the preamplifier circuit; and the mechanical saturation level can be calculated from the manufacturers' data on the maximum displacement for the EM seismometer. However, despite its importance, very little data are available on the lower level, self noise of popular EM seismometer/preamplifier combinations. This short note attempts to alleviate this situation by providing calculated generalized self-noise data for nine frequently used EM seismometers coupled with representative preamplifiers. Another use for this self-noise data is to ascertain whether a particular seismometer/preamplifier is suitable for resolving pre-event noise or low-level signals at a particular seismic site. In addition, the self noises resulting from the use of each of six seismometers with four operational amplifiers (op-amps) commonly used in seismic recorders are compared.

Self-Noise Model for an EM Seismometer/Single-Ended Preamplifier Pair

A generalized model for the signal-to-noise ratio (SNR) referred to the input for an EM seismometer operating into a single-ended preamplifier is given by Rodgers (1992, Part 1) and Rodgers (1993). This model is repeated in equation (1) below in slightly different form by the substitutions of $\omega = 2\pi f$ and $\Omega = 2\pi f_0$:

SNR

$$\text{SNR} = \frac{\left(\frac{r_d}{r_c + r_d}G\right)^2 \frac{4\pi^2 f^2}{(16\pi^4)(f_0^2 - f^2)^2 + 64\pi^4 \zeta^2 f_0^2 f^2} P_{aa}}{E_{nn} + \left(\left[\frac{r_d}{r_c + r_d}G\right]^2 \frac{4\pi^2 f^2}{[16\pi^4][f_0^2 - f^2]^2 + 64\pi^4 \zeta^2 f_0^2 f^2}\right) S_{nn}} \quad (1)$$

P_{aa} is the acceleration power density spectra (acceleration pds) of the input acceleration, E_{nn} is the generalized pds of the total electronic noise associated with the seismometer and preamplifier, and S_{nn} is the pds of the sus-

pension noise from the seismometer. The derivation and exact form for E_{nn} and the form for S_{nn} are given in the two articles by Rodgers referenced previously. The other terms in equation (1) are defined as follows: f , frequency in Hz; r_d , damping resistor in ohms; r_c , coil resistance in ohms; G , generator constant (open circuit) in V/m/sec; f_0 , resonant frequency of the spring-mass system; and ζ , damping ratio.

The expression for the SNR given in equation (1) is based on having the damping resistor in parallel with the seismometer together with a preamplifier employing an operational amplifier in the non-inverting configuration. This configuration is used because it results in a larger SNR than the other possible configurations (Rodgers, 1993).

The self noise referred to the input of the seismometer, $P_{nn.i}$, can be found from equation (1) as follows. Set the magnitude squared transfer function term of the seismometer equal to $|H(f)|^2$:

$$|H(f)|^2 = \left[\frac{r_d}{r_c + r_d} G \right]^2 \frac{4\pi^2 f^2}{[16\pi^4][f_0^2 - f^2]^2 + 64\pi^4 \zeta^2 f_0^2 f^2} \cdot \frac{V^2/\text{Hz}}{(\text{m/sec}^2)^2/\text{Hz}} \quad (2)$$

Then equation (1) becomes

$$\text{SNR} = \frac{|H(f)|^2 P_{aa}}{E_{nn} + |H(f)|^2 S_{nn}} \quad (3)$$

The SNR referred to the input of the seismometer is obtained by dividing numerator and denominator by $|H(f)|^2$

$$\text{SNR}_{\text{input}} = \frac{P_{aa}}{\frac{E_{nn}}{|H(f)|^2} + S_{nn}} \quad (4)$$

Because

$$\text{SNR}_{\text{input}} = \frac{P_{ss.i}}{P_{nn.i}} \quad (5)$$

it is clear that the signal referred to the input, $P_{ss.i}$, is given by the numerator of equation (4) and is equal to P_{aa} . Similarly, the noise referred to the input, $P_{nn.i}$, is given by the denominator of equation (4):

$$P_{nn.i} = \frac{E_{nn}}{|H(f)|^2} + S_{nn} \quad (\text{m/sec}^2)^2/\text{Hz} \quad (6)$$

The units of all the quantities referred to the input are $(\text{m/sec}^2)^2/\text{Hz}$.

Finally, substituting equation (2) into equation (6), the self noise referred to the input is found to be

$$P_{nn.i} = \frac{[4\pi^2(f_0^2 - f^2)]^2 + [8\pi\zeta f_0 f]^2}{(2\pi)^2 \left[\frac{r_d}{r_c + r_d} G \right]^2 \cdot f^2} \cdot E_{nn} + S_{nn} \quad (\text{m/sec}^2)^2/\text{Hz} \quad (7)$$

The suspension noise, S_{nn} , is given by

$$S_{nn} = 16\pi \frac{kT\zeta f_0}{M} \quad (\text{m/sec}^2)^2/\text{Hz} \quad (8)$$

where k is Boltzmann's constant and T is the room temperature in degrees Kelvin.

The generalized total electronic noise, E_{nn} , is

$$E_{nn} = V_{00} \left(\frac{f_{cv}}{f} + 1 \right) + I_{00} \left(\frac{f_{ci}}{f} + 1 \right) r_p^2 + 4kTr_p \quad \text{V}^2/\text{Hz} \quad (9)$$

In equation (9), r_p is the parallel combination of r_c and r_d . The two resistances that set the gain of the operational amplifier-based preamplifier are assumed to be low values compared to r_p and thus do not appear in E_{nn} . This is the proper strategy to follow to achieve minimum electronic noise. It may be difficult to achieve with a low-resistance seismometer but it serves well as a limiting case here permitting a generalized form for E_{nn} . V_{00} and I_{00} are the high-frequency levels of the op-amp voltage and current noise pds's, respectively. The corner frequencies for the voltage and current noise pds's are f_{cv} and f_{ci} , respectively. As mentioned earlier, complete details regarding S_{nn} and E_{nn} and the SNRs for various seismometer and circuit configurations are given in the two previously cited articles.

Seismometer and Amplifier Parameters

The instrumental parameters for the nine common EM seismometers being considered are given in Table 1, ordered in terms of resonant frequency. They range from the Oyo-Geospace HS-1 geophone to the long-period Teledyne-Geotech SL-210V and SL-220H. Four of the nine seismometers treated have 1-Hz resonant frequencies.

Two different operational amplifiers are used in these calculations, the high noise resistance linear technology LT1012 for the high coil resistance GS-13, and the lower noise resistance precision monolithics OP-27 for the remaining lower coil resistance seismometers. Noise resistance, R_n , is defined as the square root of the ratio of the voltage noise pds, V_{nn} , to the current noise pds, I_{nn} . The noise data on the LT1012 and the OP-27 operational amplifiers are given in Table 2. They are a good but not

exact match to the seismometers. It is shown in Rodgers (1993) how to exactly match the operational amplifier and seismometer to achieve the maximum SNR over the entire passband, which requires a FET-based or FET-like op-amp. Although the bipolar LT1012 and OP-27 cannot do this, they are used for these computations because they represent the common current practice and so are felt to make the self-noise data more useful.

Plots of Self-Noise Spectra

Using equation (7) together with equations (8) and (9), the self-noise spectra referred to the input are computed for the nine seismometers listed in Table 1. The nine self-noise spectra are shown in Figures 1 and 2. In Figure 1, the spectra are given as spectral densities (per Hertz). To increase the utility of the data, the same curves are given in three different sets of units: amplitude density spectra (in $\text{m/sec}^{**2}/\text{Hz}^{**0.5}$), power density spectra (in $\text{m/sec}^{**2}^{**2}/\text{Hz}$) and in decibels (re $1 \text{ m/sec}^{**2}/\text{Hz}^{**0.5}$ for the amplitude density spectra and re $\text{m/sec}^{**2}^{**2}/\text{Hz}$ for the power density spectra). Because of the definition of decibels, this results in the same numerical decibel value for both sets of units. The decibel values are given on the right-hand scale of Figure 1. Peterson's Low Model, labeled LNM (Peterson, 1982; Peterson and Hutt, 1982; Peterson and Tilgner, 1985; Peterson and Hutt, 1989), is included for comparison

purposes. All of the self-noise curves have a vee shape with a minimum at the resonant frequency, f_0 , of the seismometer. The reason for this can be seen in equation (6), which shows that the shape of $P_{nn,i}$ results from dividing the relatively constant noise term, E_{nn} , by the magnitude squared transfer function term, $|H(f)|^2$, which has the shape of an inverted vee with a maximum at f_0 .

Because Figures 1 and 2 contain so many curves, self-noise spectra for the horizontal components were omitted because they were nearly identical to those of the vertical components. The omitted horizontal components are the Kinometrics SH-1 and the Teledyne-Geotech SL-220H. In addition, the self noises of the Kinometrics SS-1 and the Mark Products L-4C were very similar and are shown as one curve. Actually, the SS-1 is about 20% less noisy than the L-4C. The levels of the nine self-noise curves are as expected, with the weak motion seismometers being the quietest and the noise levels rising as the curves progress toward the higher frequency, lower generator constant geophones.

To give the self-noise data in real (nonspectral density) units, the data in Figure 1 is presented again in Figure 2 in rms meters in a one-half octave bandwidth. This conversion uses the relationship (Aki and Richards, 1980):

$$\text{rms} = \sqrt{2 \cdot BW(f) \cdot P_{nn,i}}, \quad (10)$$

Table 1
Instrumental Parameters for Nine EM Seismometers

Seismometer type	f_0 , Hz	G , V/m/sec	ζ	M, kg	r_c , Ohms	r_d , Ohms
Oyo-Geospace HS-1	4.5	62.2	0.6	0.0227	2,500	7,500
Mark Product L-22D	2.0	112.0	0.8	0.0728	5,470	14,300
Sprengnether S-6000CD	2.0	373.3	0.6	0.5	10,000	11,000
Mark Products L-4C	1.0	276.4	0.7	1.0	5,500	8,900
Kinometrics SS-1	1.0	345.0	1.0	1.45	5,000	6,530
Teledyne-Geotech S-13	1.0	629.0	1	5.0	3,600	6,300
Teledyne-Geotech GS-13	1.0	2150	1	5.0	8,900	74,500
Kinometrics SV-1	0.2	270	1	1.0	3,800	22,000
Teledyne-Geotech SL-210V	0.05	90	1	2.0	1,200	6,440

Table 2
Noise Parameters for the LT1028, OP-27, OP-227, OP77 and LT1012 Operational Amplifiers

Operational amplifier	V_{00} , V^2/Hz	f_{cv} , Hz	I_{00} , A^2/Hz	f_{ci} , Hz	R_0 , Ohms
Linear Technology, LT1028	7.2×10^{-19}	3.5	8.1×10^{-25}	250	943
Precision Monolithics, OP-27	9.0×10^{-18}	2.7	1.6×10^{-25}	140	7,500
Precision Monolithics, OP-227	9.0×10^{-18}	2.7	1.6×10^{-25}	140	7,500
Precision Monolithics, OP-77	1×10^{-16}	2.0	6×10^{-26}	200	41 K
Linear Technology, LT1012	1.96×10^{-16}	2.5	3.6×10^{-29}	120	2.3 M

*Listed in order of increasing R_0 . Values are R_0 is the level of the noise resistance at high frequencies ($f \gg f_{ci}$) and is given by $R_0 = \sqrt{V_{00}/I_{00}}$

where the expression for the bandwidth, $BW(f)$, is given by equation (11) with $n = 2$, as

$$BW(f) = (2^{1/2n} - 2^{-1/2n}) \cdot f. \quad (11)$$

Equation (11) corrects equation (2) in Rodgers (1992, Part 1).

The self-noise curves in Figure 2 are similar to those in Figure 1 but are rotated counterclockwise by half a unit of slope due to the multiplication by the square root of f , which occurs when equation (11) is substituted into equation (10). The data from Figure 2 can be used to calculate the dynamic range of a particular seismometer/preamplifier pair as described at the beginning of this article. Because the upper clipping or saturation level is a zero-to-peak value, to determine the dynamic range, the self noise must also be put in the same units of zero-to-peak values. This can be done using equation (12) of Taylor (1981):

$$\text{zero-to-peak} = 3 \times \text{rms} \quad (12)$$

Self-Noise Model for an EM Seismometer/ Differential Preamplifier Pair

Seismic data recorders all use differential (double-ended) analog input stages to reject common mode sig-

nals. The self-noise model for an EM seismometer differential preamplifier configuration is nearly the same as that for a single-ended configuration with only the total electronic noise being different. The total electronic noise, E_{nm} , for the differential preamplifier configuration is nearly twice that of the single-ended configuration (Rodgers, 1993). This can be seen from equation (9) where, for the differential configuration, V_{00} and I_{00} are doubled but $4kTr_p$ remains the same. However, in an actual circuit, the noise in the differential preamplifier is also reduced by its ability to reject common mode noise such as that picked up by connecting cables. The self-noises for six EM seismometers operating into differential input stage preamplifiers using four different differential op-amps are computed using equation (9), in which the terms V_{00} and I_{00} in equation (7) are doubled.

Of the nine seismometers treated in the previous section, only six are considered here: the HS-1, L-22D, L-4C, GS-13, SV-1, and the SL-210V. The SS-1 is similar to the L-4C, and the S-13 is nearly the same as the GS-13 but with an amplitude density spectra self-noise level almost exactly twice that of the GS-13. The op-amps used in the computations are the Linear Technology LT1028 and LT1012 and the Precision Monolithics, Inc., (PMI) OP-227 and OP-77, both of which are differential op-amp pairs mounted on a single chip. Their noise parameters are given in Table 2. The PMI OP-227 is used in

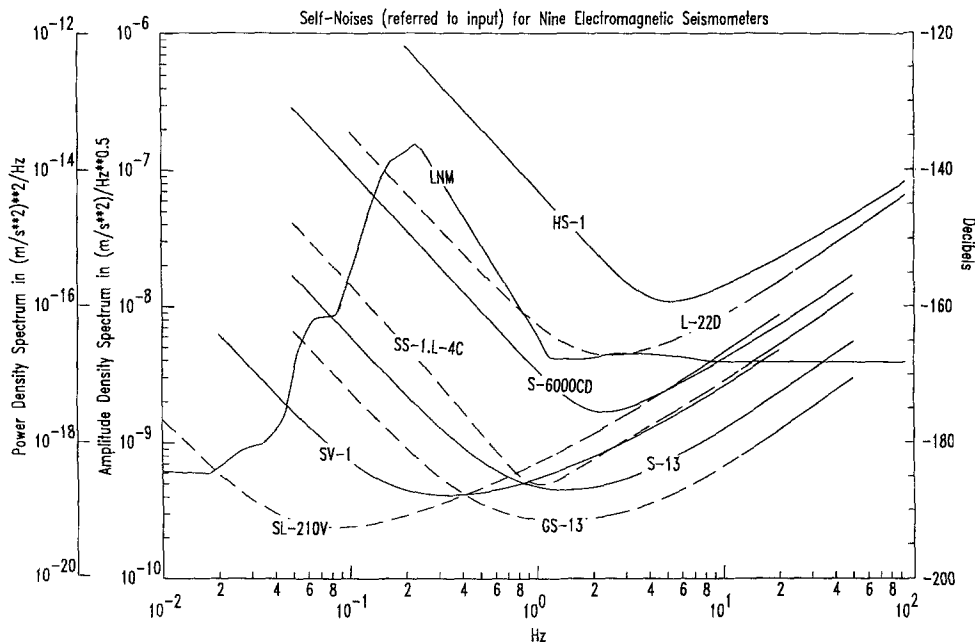


Figure 1. Calculated self-noise spectral densities, referred to the input, of nine electromagnetic seismometers are shown in three sets of units: amplitude density spectra (in $m/sec^{**2}/Hz^{**0.5}$), power density spectra (in $m/sec^{**2}^{**2}/Hz$), and in decibels re one unit of each of the above two quantities. Peterson's LNM is included for comparison. The GS-13 is operating into the LT1012 op-amp. The remaining eight seismometers are operating into the PMI OP-27 op-amp. The op-amps are assumed to be in the noninverting configuration with the damping resistors in parallel with the seismometer coil terminals.

the analog input stage of the Refraction Technology REF TEK 72A-07. The PMI OP-77 is used in the input stages of the Teledyne-Geotech PDAS-100 and the USGS GEOS-I. The REF TEK low-noise preamplifier module used with the REF TEK 72A-02 uses two LT1012s in a differential configuration (Menke *et al.*, 1992). The QPREAMP used for connecting EM seismometers to the Quanterra, Inc., Quantagator Q680 uses two OP-27s also in a differential configuration. Several recorders, such as the REF TEK 72A-02 and -06 and the Kinematics SSR-1, use the PMI AMP-01 differential op-amp in their input stage. The manufacturer, PMI, does not publish the current noise spectrum for this component, so the AMP-01 could not be included in these computations.

Self-Noise Spectra for Six Seismometers with Four Op-Amps

Self-noise spectra for the HS-1, L-22D, and the L-4C paired with the LT1028, OP-227, OP-27, and the LT1012 op-amps are given in Figures 3(a), 3(b), and 3(c). The file names are given in the lower right-hand corner of the plots and are listed with the quietest on the bottom and the noisiest on top. The units are amplitude density spectra (in $\text{m/sec}^{**2}/\text{Hz}^{**0.5}$). Amplitude density spectra (ads) rather than pds are used because ads relates

directly to data amplitude. As in Figures 1 and 2, Peterson's Low Noise Model (labeled LNM) is included as a reference.

As shown in Figure 3(a), the HS-1 is quietest when paired with the OP-227 and noisiest with the LT1012. The reason for this is that the noise resistance of the LT1012 is much too high at all frequencies to match the 7.5 K-Ohm coil resistance of the HS-1. A detailed development and discussion of matching a seismometer and preamplifier to achieve the maximum signal-to-noise ratio (SNR), and the lowest self noise is given in Rodgers (1993). The L-22D and L-4C shown in Figures 3(b) and 3(c), respectively, are also both quietest with the OP-227 but are noisiest with the very low noise resistance LT1028. The reason for this is that the mismatch with the very low noise resistance LT1028 is worse than the mismatch with the very high noise resistance LT1012. Both the L-22D and the L-4C are about 20% more noisy with the OP-77 than the OP-227.

A different situation is shown in Figure 4(a) for the very high coil resistance and generator constant GS-13. It has its lowest self noise with the high noise resistance LT1012, although it is almost as quiet, with the OP-227 and OP-77. The self-noise spectra for the SV-1 are shown in Figure 4(b), in which it is seen that the comparative results are similar to those for the L-22D

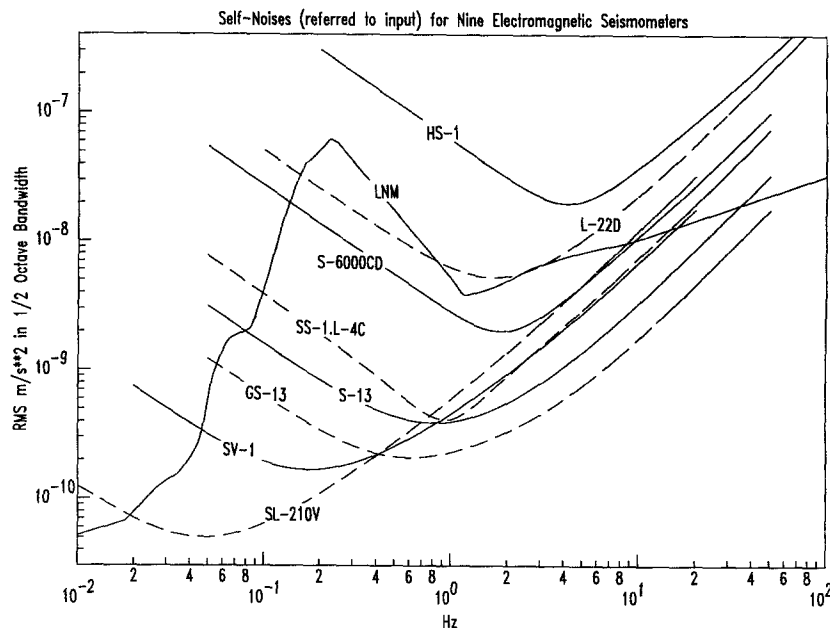


Figure 2. Calculated self-noise spectra, referred to the input, for nine electromagnetic seismometers are given in rms meters in a one-half octave bandwidth. The curves are similar to those of Figure 1 but are rotated counterclockwise by one-half a unit of slope because of the one-half octave bandwidth assumption. Peterson's LNM is included as in Figure 1. The GS-13 is operating into the LT1012 op-amp. The remaining eight seismometers are operating into the PMI OP-27 op-amp. The op-amps are assumed to be in the noninverting configuration with the damping resistors in parallel with the seismometer coil terminals.

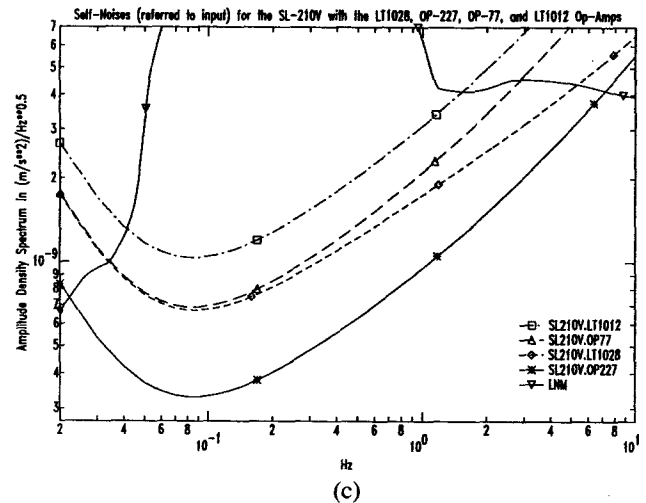
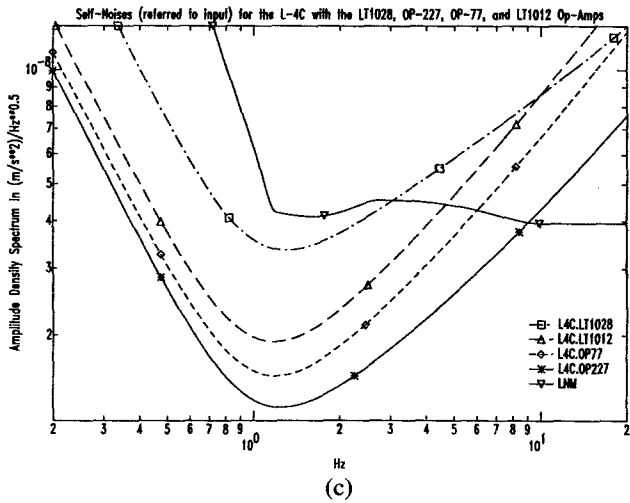
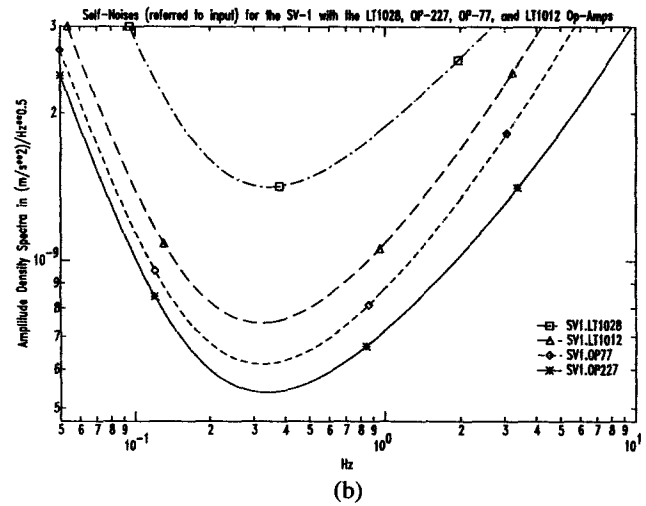
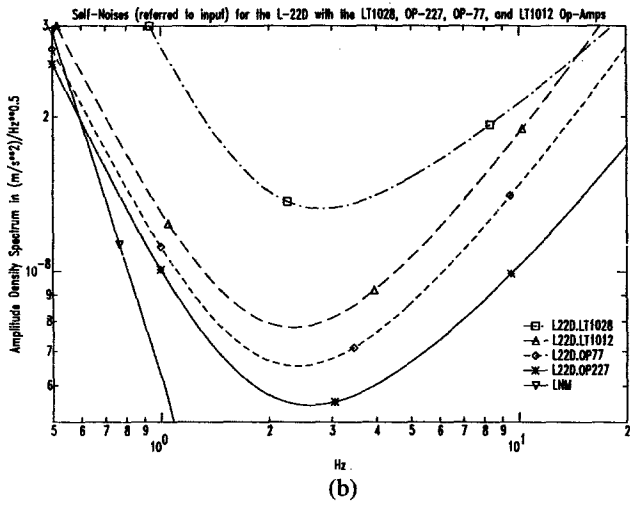
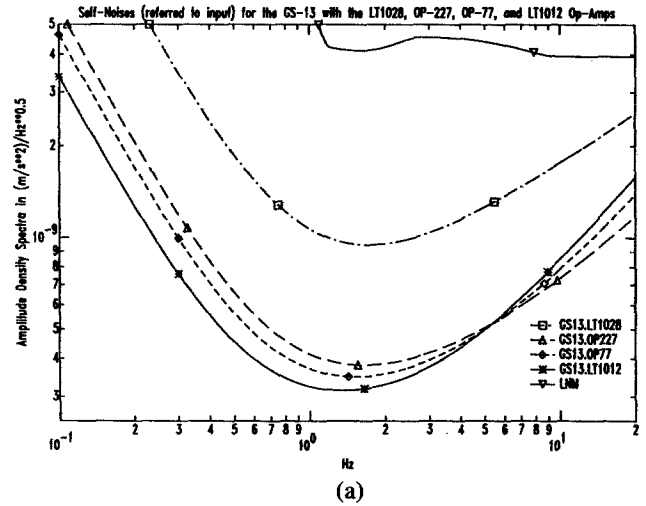
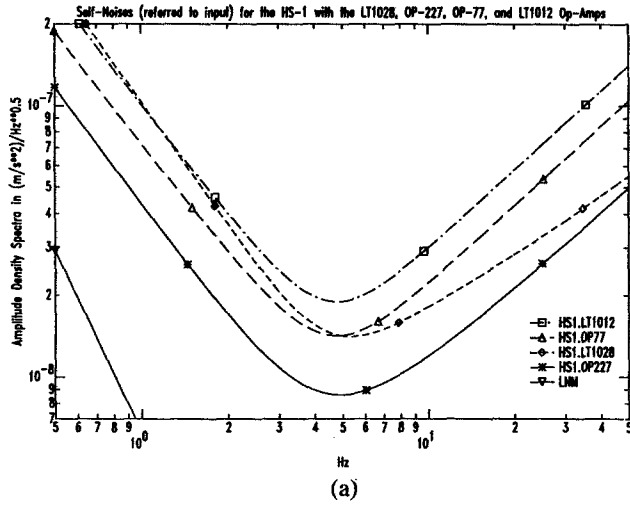


Figure 3. Calculated self-noise spectra for the HS-1, L-22D, and L-4C seismometers paired with the LT1028, OP-227, OP-77, and LT1012 operational amplifiers. The units are amplitude density spectra (in $m/sec^2/Hz^{0.5}$). The file names are ordered in terms of self noise with the noisiest on the top. Peterson's Low Noise Model (LNM) is included for comparison.

Figure 4. Calculated self-noise spectra for the GS-13, SV-1, and SL-210V seismometers paired with the LT1028, OP-227, OP-77, and LT1012 operational amplifiers. The units are amplitude density spectra (in $m/sec^2/Hz^{0.5}$). The file names are ordered in terms of self noise with the noisiest on the top. Peterson's Low Noise Model (LNM) is included for comparison.

and L-4C, although the absolute self-noise levels are much lower.

Finally, the spectra in Figure 4(c) for the long period, low coil resistance SL-210V show that it is very much more quiet (by a factor of 3) with the OP-227 than the LT1012. Furthermore, the SL-210V is twice as quiet with the OP-227 as with either the LT1028 or the OP-77.

The conclusion to be drawn from Figures 3(a), 3(b), and 3(c) and 4(a), 4(b), and 4(c) is that when connecting an EM seismometer to a seismic recorder, for minimum noise it is important to consider the op-amp used in the analog front end of the recorder. The PMI OP-27 or OP-227 appear to be good general choices, except when using the GS-13.

Acknowledgments

The author acknowledges supportive discussions with Tom McEvilly of the University of California at Berkeley, and the support of Phil Harben and Fred Followill of Lawrence Livermore National Laboratory. Kinometrics, Quanterra, Refraction Technology, Teledyne Geotech, and the U.S.G.S., Menlo Park, generously shared details and component information on the analog front ends of their digital recorders.

The author also acknowledges support from the Southern California Earthquake Center under Contract Number 572726 and the Lawrence Livermore National Laboratory under DOE Contract W-7405-Eng-48.

References

Aki, K. and P. Richards (1980). *Quantitative Seismic Theory and Methods*, W. H. Freeman, San Francisco, Calif.

- Peterson, J. (1982). GDSN enhancement studies final report. ARPA Order No. 4259, USGS Albuquerque Seismological Laboratory, Albuquerque, New Mexico. November.
- Peterson, J. and C. Hutt (1982). *Test and Calibration of the Digital World-Wide Standardized Seismograph*, U.S. Geol. Surv. Open-File Rep. 82-1087.
- Peterson, J. and C. Hutt (1989). *IRIS/USGS Plans for Upgrading the Global Seismographic Network*, U.S. Geol. Surv. Open-File Rep. 89-471.
- Peterson, J. and E. T. Tilgner (1985). *Description and Preliminary Testing of the CDSN Sensor Systems*, U.S. Geol. Surv. Open File Rep. 85-288.
- Rodgers, P. W. (1992). Frequency limits for seismometers as determined from signal-to-noise ratios. Part 1, the Electromagnetic seismometer, *Bull. Seism. Soc. Am.* **82**, 1071-1098.
- Rodgers, P. W. (1993). Maximizing the signal-to-noise ratio of the electromagnetic seismometer: the optimum coil resistance, amplifier characteristics, and circuit, *Bull. Seism. Soc. Am.* **83**, no. 2, 561-582.
- Taylor, S. (1981). Properties of ambient seismic noise and summary of noise spectrum in the vicinity of RSTN sites, Lawrence Livermore National Laboratory, Livermore, Calif., UCID-18928.
- Menke, W., L. Shengold, and B. Busby (1992). Precision of broadband velocity measurements made with IRIS/PASSCAL instrumentation, *Bull. Seism. Soc. Am.* **82**, 2256-2262.

Lawrence Livermore National Laboratory
P.O. Box 808
Livermore, California 94550
and
Institute for Crustal Studies
University of California
Santa Barbara, California 93106-1100

Manuscript received 11 May 1993.